
A New Two Switch Non-Inverted Buck-Boost Converter for PV System

*¹J.N. Bhanutej, ²U. Hemalatha, ³B. Nagi Reddy

*^{1,2,3}Vignana Bharathi Institute of Technology, Hyderabad, India
Email: bhanutej.mtech@gmail.com, udarihmalatha@gmail.com

Abstract

For photovoltaic-based systems, this study suggests a quadratic buck-boost converter with two active switches. The reduced redundant power processing (R^2P^2) concept serves as the foundation for the suggested converter. To achieve quadratic voltage gain, conventional boost and buck-boost cells are arranged in a non-cascading fashion. In order to obtain a high voltage conversion ratio and a low component count, the two active switches of the proposed converter operate concurrently. The effect on converter performance is also evaluated once the converter has been tested with varied sources and loads. Here, the voltage conversion ratio and semiconductor stresses of the proposed converter are described. Under steady-state conditions, the proposed converter's precise performance is assessed. With the help of MATLAB/SIMULINK, the suggested converter is evaluated.

Keywords. Two switch, PV, buck-boost, non-inverting, dc-dc converter.

1. INTRODUCTION

The proliferation of mobile systems and equipment over the past several decades has spurred innovation in portable power supply systems. This includes anything from powering IoT devices to overseeing renewable energy production. Increases in efficiency, conversion ratios, and power density are only some of the additional requirements placed on power electronics systems as a result of the industry's present direction. Because of its ability to process energy with the help of appropriate control schemes, the switching converter is essential to any contemporary power supply system [1].

In this regard, the design of novel switching converter topologies, as well as novel

converter connectivity architectures and/or methods, is of interest. Similarly, low-voltage and/or low current semiconductor components are of relevance for this use. Numerous high transformation-ratio topologies based on isolated and nonisolated techniques have been devised recently, with implementation depending largely on the desired use case. Total harmonic distortion (THD) reduction, power factor improvement, output voltage control, and energy efficiency are some of the primary goals of switching converter-based AC power supply systems [2]. For these uses, it is preferable that the converter's output and input power supplies be completely isolated from one another. The first is the increasing need for DC power systems to serve portable and electronic devices, and the second is the development of DC power systems. Subsequently the voltage levels produced by fuel cells, solar systems, and/or batteries are just a few tens of volts, switching converters need to have high conversion ratios [3]. The ability to process energy at hundreds of volts, with or without galvanic separation, is necessary for this state to exist.

Recently, there has been a rise in interest for switching converters that can regulate the input voltage to meet the needs of certain devices. With the goal of achieving a low output voltage and a high-power factor. After introducing the quadratic buck & simple boost configurations [4], synthesized a switching converter that could be used in a solar system to modify the energy being fed into an inverter. As switching converter technology has advanced, converters with floating loads have emerged, limiting their usefulness. As an added bonus, certain circuit synthesis topologies merge the characteristics of quadratic converters with those of fundamental topologies [5]. Emergent topologies are being developed to solve real-world problems encountered by power supply for renewable energies systems [6]. This work introduces a non-cascade architecture for connecting basic converters as a switching converter configuration, based on the reduced redundant power processing approach. The output voltage is both multiplicatively increased and decreased, defining the achieved conversion ratio. The suggested converter has a low number of parts, produces a noninverting voltage at its output, shares a node with its input, and can accept a constant current input. The effect of the PV system on the converter's functioning is also studied by analyzing it with various source and load configurations.

2. PROPOSED NON-INVERTED BUCK-BOOST CIRCUIT

Block A's boost network with reversed output polarities is seen in Figure 1.a. This boost network causes storage element C1's voltage polarity to be reversed, which results in a negative voltage at block B's input port. The output port of the I-IIA structure is then supplied with a positive voltage by a buck-boost

network, as seen in Figure 1.b. Furthermore, E denotes the voltage source, while R denotes the load.

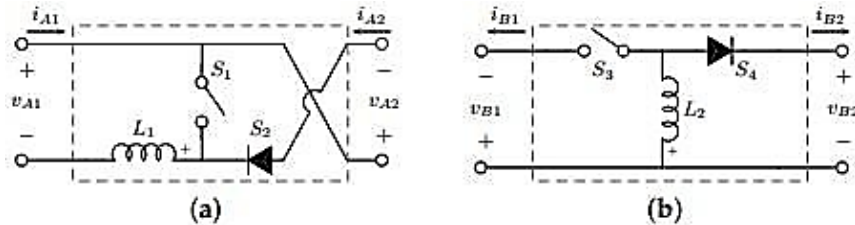


Figure 1. Basic switching cells that are not isolated: (A) buck-boost; (B) boost

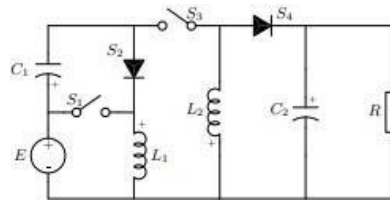


Figure 2. Proposed wide range buck-boost network

As previously mentioned, this kind of non-cascaded construction has been utilized to create various high-gain or secondary voltage conversion ratio devices topologies for PV applications. Nonetheless, there are several methods for designing topologies with specific high voltage gains. The planned converter steady-state analysis is expanded in this section by connecting the converter's inputport to a voltage source. The contributions of PV modules and converters are discussed in the following subsections. The states of the active switches define the converter's operating modes, and these assumptions are made:

- The converter is running continuously (CCM).
- To achieve high voltage gain, active switches S1 and S3 operate synchronously.
- The switching function q describes the mode of operation of active switches. An equation provides them (1).

$$q = \begin{cases} 1 & \rightarrow 0 < t \leq t_{on} \\ 0 & \rightarrow t_{on} < t \leq T_s \end{cases} \quad q = \begin{cases} 0 & \rightarrow 0 < t \leq t_{on} \\ 1 & \rightarrow t_{on} < t \leq T_s \end{cases} \quad (1)$$

T_s denote the switching period, and T_{on} denotes the active switch conducting time. The converter's operating modes are indicated by the on- and off states of the active switches. In this situation, capacitor C1 powers load R while capacitor C2 powers inductor L2. The differential equations characterize the system's behaviour in this mode of operation:

$$L_1 \frac{di_{L1}}{dt} = E, \quad (2)$$

$$L_2 \frac{di_{L2}}{dt} = V_{C1} - E \quad (3)$$

$$C_1 \frac{dv_{C1}}{dt} = -i_{L2} \quad (4)$$

$$C_2 \frac{dv_{C2}}{dt} = -\frac{V_{C2}}{R} \quad (5)$$

Inductor L1 delivers energy to capacitor C1 via diode S2, and inductor L2 sends energy to the capacitors R-C2 via diode S4 while the switches are off (Figure 3b). The relevant differential equations are as follows:

$$L_1 \frac{di_{L1}}{dt} = E - V_{C1} \quad (6)$$

$$L_2 \frac{di_{L2}}{dt} = V_{C2}, \quad (7)$$

$$C_1 \frac{dv_{C1}}{dt} = -i_{L1} \quad (8)$$

$$C_2 \frac{dv_{C2}}{dt} = i_{L2} - \frac{V_{C2}}{R} \quad (9)$$

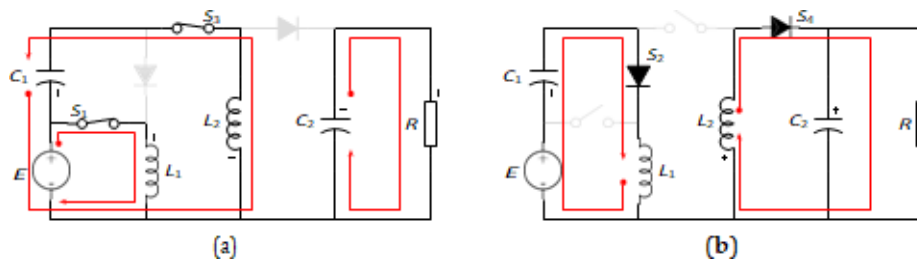


Figure 3. The proposed converter has 2 operating modes: q equals 1 in (a) and 0 in (b).

During one switching period, the voltages at the inductors' terminals and currents through the capacitors are defined by Equations (2) and (3). Equations (4) and (5) describe the converter's steady-state operation using the concepts of volt second and charge balances are applied to these voltages and currents (5).

$$\int_0^{T_s} v(t) dt = 0 \quad (10)$$

$$\int_0^{T_s} i(t) dt = 0 \quad (11)$$

$$I_{L1} = \frac{ED^3}{(1-D)^4 R} \quad (12)$$

$$I_{L2} = \frac{ED^2}{(1-D)^3R} \quad (13)$$

$$V_{C1} = \frac{E}{(1-D)}, \quad (14)$$

$$V_{C2} = \frac{ED^2}{(1-D)^2} \quad (15)$$

Where D is the converter's nominal duty ratio, the converter's voltage gain becomes quadratic with respect to duty ratio at that point, indicating a wide range of output step-up or step-down voltage conversion characteristics. Equation represents the voltage gain as a result (10). The steady-state operating condition and the voltage conversion ratio are the only applicable when the converter is in CCM mode. The conversion ratio is also positive, and the ports for input and output are both grounded.

$$M = \frac{V_{C2}}{E} = \frac{D^2}{(1-D)^2} \quad (16)$$

3. RESULTS

Finally, simulation of the converter in MATLAB/Simulink is done to obtain the response.

Table 1 Simulation values

Parameters or components	values
Input voltage (Vin)	24v
Output voltage (Vo)	200v
Output power (Po)	200W
Switching frequency (Fs)	80 KHz
Load resistance	200Ω
Duty ratio	0.7426
M(D)	8.32
L1(α=0.5A)	29.55 μH
L2(α=0.5A)	331.2 μH
C1(Δ=2V)	4.64 μF
C2(Δ=2V)	4.64 μF

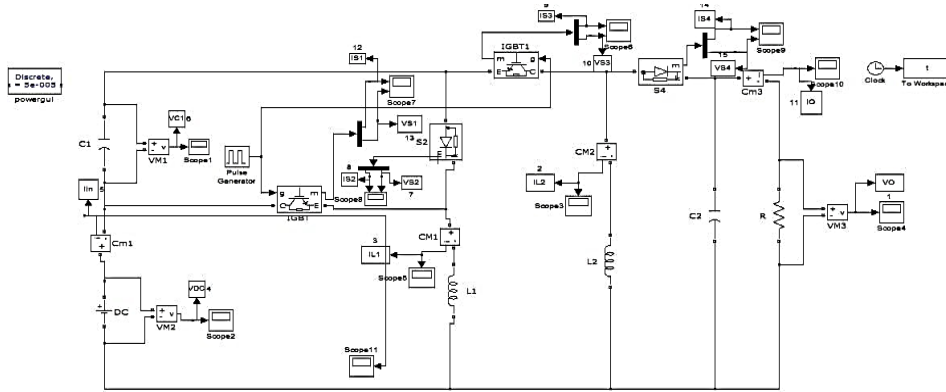
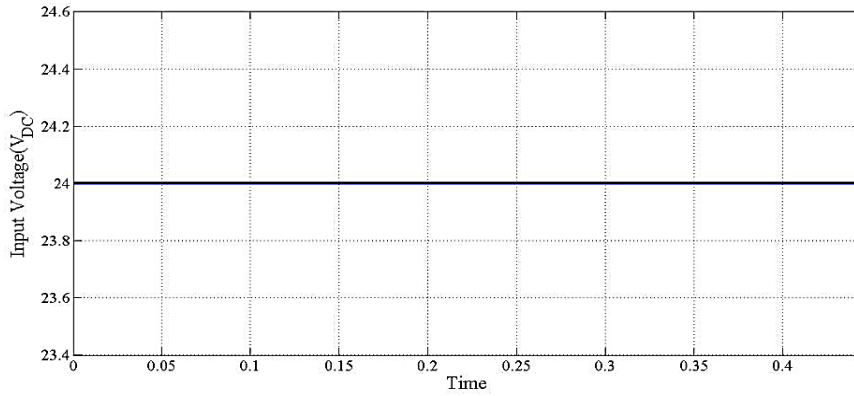
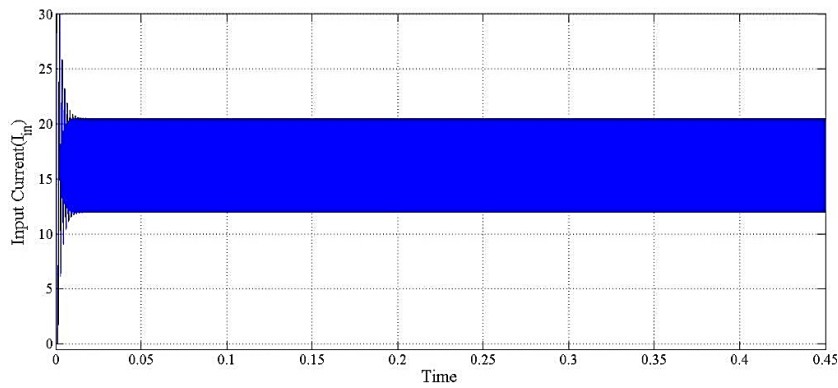


Figure 4. Simulation model

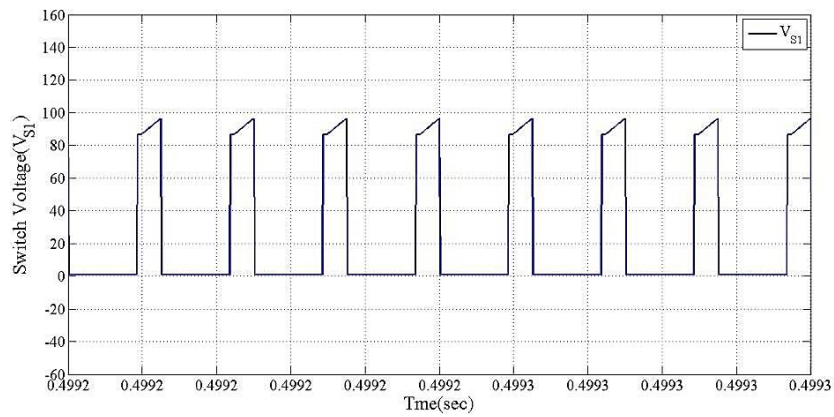


(a)

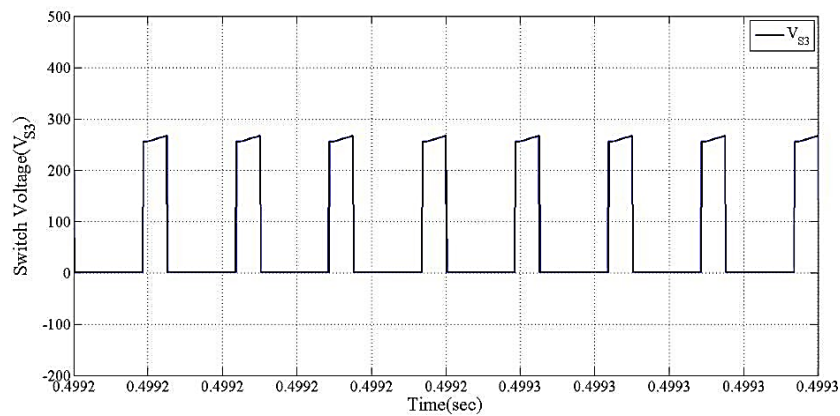


(b)

Figure 5. Input voltage and current



(a)



(b)

Figure 6. Switching voltages

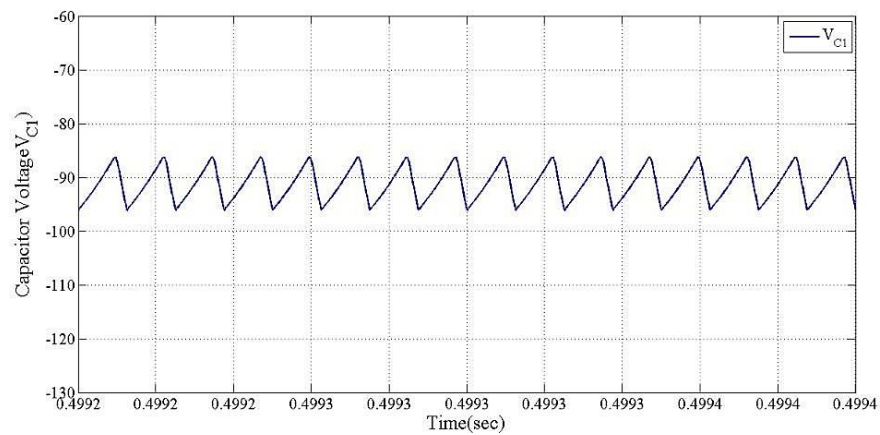
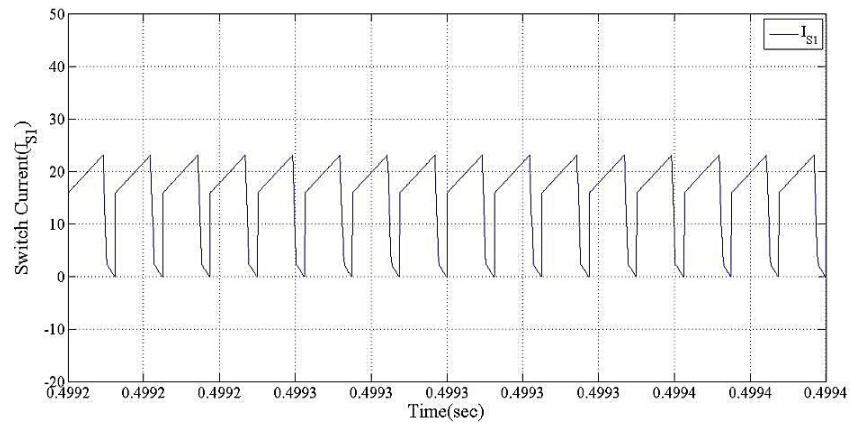
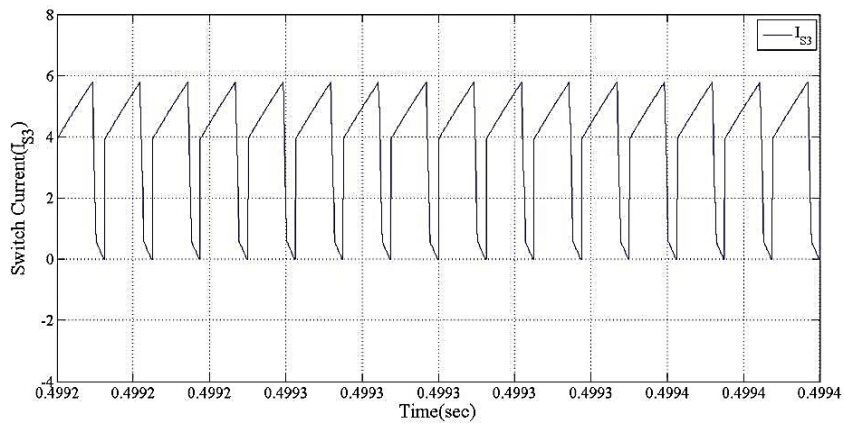


Figure 7. Capacitor voltage



(a)



(c)

Figure 8. Switching currents

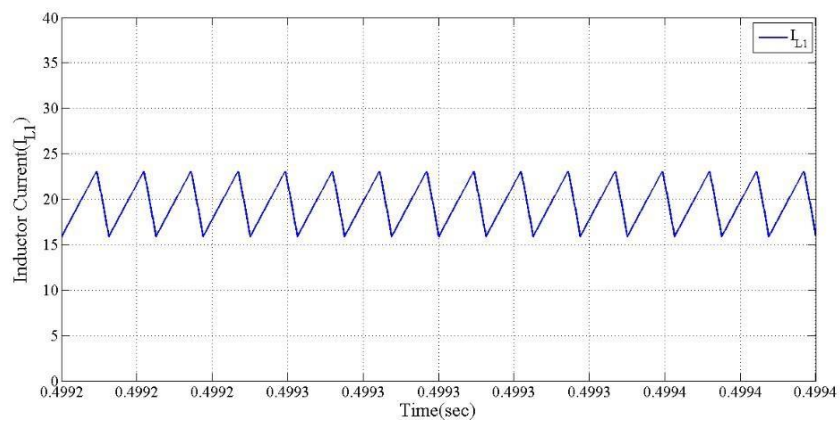
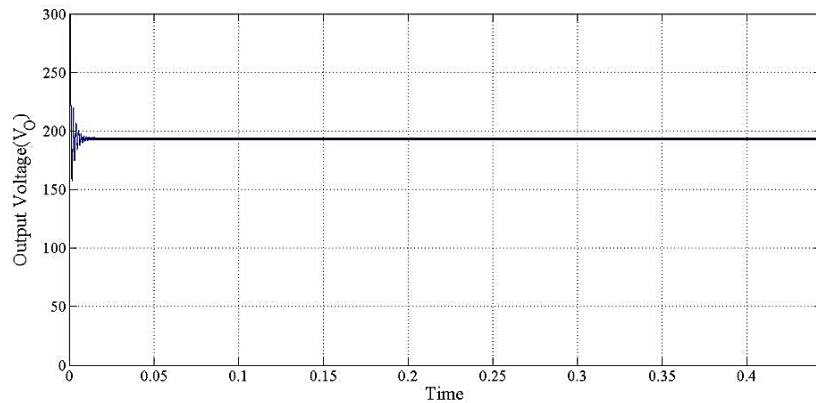
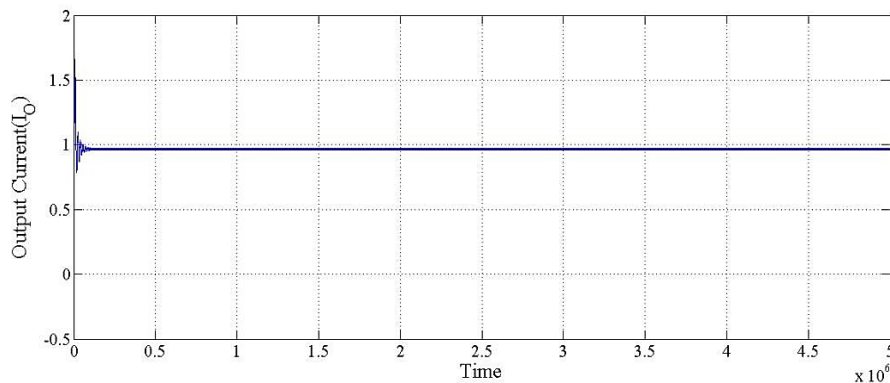


Figure 9. Inductor currents



(a)



(b) Output current

Figure 10. Output voltage and current

Global solar radiation varies greatly depending on fog. This is especially relevant to the amperage and power produced. The complexity of the P&O calculation will change the voltage at the PV module's terminals in tests; efficacy was greater than 80%. Using large components like SiC semiconductors and techniques like cooperative correction, in particular, will boost the effect. Nevertheless, replication evaluations were performed in this work to support hypothetical results regarding conversion rates, behavior, and potential use in PV applications. The mimicked response clearly predicted a strong response from the model converter and confirmed the correctness of the generated model.

4. CONCLUSION

In this article, a quadratic buck-boost converter that is based on the connection of two fundamental switch cells in an uncascaded design. Because the converter correctly connects PV devices to DC system connections, this is suitable for PV applications. PV applications behave differently than voltage source applications,

according to steady-state analysis. The voltage stress on the semiconductor is further greater in PV applications, but the current stress is lower. The simulation results show that the converter behaves properly under real-world conditions, with the duty cycle controlling the voltage at the PV module terminals and regulating the power produced. The converter has a high voltage conversion ratio, which enables it to handle wide input voltage swings while keeping the output voltage clamped. Inverters are suitable for grid-connected or micro-grid applications.

5. REFERENCES

- [1] Alonge, F.; Pucci, M.; Rabbeni, R.; Vitale, G. Dynamic modelling of a quadratic DC/DC single-switch boost converter. *Electr. Power Syst. Res.*, 152, 130–139, 2017.
- [2] Ozdemir, S.; Altin, N.; Sefa, I. Fuzzy logic based MPPT controller for high conversion ratio quadratic boost converter. *Int. J. Hydrogen Energy*, 42, 17748–17759, 2017.
- [3] Nagi reddy. B, sahithipriya. Kosika, manishpatel. Gadam, jagadhiswar. Banoth, ashok. Banoth, srikanthgoud. B, “Analysis of positive output buck-boost topology with extended conversion ratio”, *Journal of Energy Systems*, 6(1), pp. 62–83, 2022.
- [4] Al-Saffar, M.A.; Ismail, E.H.; Sabzali, A.J. Integrated buck-boostquadratic buck PFC rectifier for universal input applications. *IEEE Trans. Power Electron.*, 24, 2886–2896, 2009.
- [5] Zhang, N.; Zhang, G.; See, K.W.; Zhang, B. A single-switch quadratic buck-boost converter with continuous input port current and continuous output port current. *IEEE Trans. Power Electron.*, 33, 4157–4166, 2018.
- [6] Gorji, S.A.; Mostaan, A.; My, H.T.; Ektesabi, M. Non-isolated buck-boost DC-DC converter with quadratic voltage gain ratio. *IET Power Electron.*, 12, 1425–1433, 2019.
- [7] Nagi Reddy, B., Chandra Sekhar, O., Ramamoorthy, M. “Analysis and implementation of single-stage buck-boost-buck converter for battery charging applications *Journal of Advanced Research in Dynamical and Control Systems*, 2018, 10(4), pp. 446–457.